Traffic flow optimization on roundabouts

Legesse Lemecha Obsu, Maria Laura Delle Monache, Paola Goatin, Semu Mitiku Kassa

Traffic flow optimization on roundabouts

Legesse L. Obsu*, Maria Laura Delle Monache†,
Paola Goatin†and Semu M. Kassa*

Abstract

The aim of this article is to propose an optimization strategy for traffic flow on roundabouts using a macroscopic approach. The roundabout is modeled as a sequence of 2×2 junctions with one main lane and secondary incoming and outgoing roads. We consider two cost functionals: the total travel time and the total waiting time, which give an estimate of the time spent by drivers on the network section. These cost functionals are minimized with respect to the right of way parameter of the incoming roads. For each cost functional, the analytical expression is given for each junction. We then solve numerically the optimization problem and show some numerical results.

Keywords: Traffic problems; Conservation laws; Macroscopic models; Riemann problem; Optimal Control

MOS subject classification: 90B20; 35L65; 49J20

1 Introduction

The first macroscopic model of traffic flow is due to Lighthill and Whitham [1] and independently, Richards [2]. They proposed a fluid dynamic model for traffic flow on a single infinite road, using a non-linear partial differential equation (PDE). This is commonly referred as the LWR model. More recently, several authors proposed models on networks that are able to describe the dynamics at intersections, see [3, 4, 5, 6] and references therein. These models consider different types of solutions and some of them have been used for optimization of traffic flow of networks, see for example [7, 8, 9, 10, 11].
In this article, we focus on optimization problems for roundabouts. We consider the model introduced in [5] and apply it to roundabouts. Roundabouts can be seen as particular road networks and they can be modeled as a concatenation of junctions. Here, we focus on roundabouts with three entrances and three exits that can be modeled as a concatenation of 2x2 junctions with two incoming and two outgoing roads, but the approach can be generalized to more general networks. In particular, each junction has one incoming main lane, one outgoing main lane and a third link with incoming and outgoing fluxes. The third road is modeled with a vertical buffer of infinite capacity for the entering flux and with an infinite sink for the exiting one. The main lane evolution is described by a scalar hyperbolic conservation law, whereas the buffer dynamics is described by an ordinary differential equation (ODE) which depends on the difference between the incoming and outgoing fluxes on the link. The outgoing secondary road is modeled as a sink. At each junction, the Riemann problem is uniquely solved using a right of way parameter, and solutions are constructed exactly via wave-front tracking method. For details on the wave-front tracking method we refer the reader to [12].
Our aim is to optimize some cost functionals, such as the Total Travel Time (TTT) and the Total Waiting Time (TWT) through a suitable choice of the right of way parameter for incoming roads. The TTT and the TWT give an estimate of the time spent by drivers in the network sections or in the queues at the buffers, respectively. The cost functionals are computed analytically on a single 2x2 junction. Then, the traffic behavior for the whole roundabout is studied numerically using local optima. Numerical simulations show the effectiveness of the optimization strategy, compared to the case of fixed constant right of way parameters. The article is structured as follows. In Section 2 we describe the junction model and the roundabout model. In section 3 we give the solution of the Riemann Problem. In Section 4 we

*University of Addis Ababa, Ethiopia
†Inria Sophia Antipolis, France

describe the cost functionals and compute local optimal priority parameters. Section 5 and 6 are devoted to the description of the numerical scheme and to numerical tests.

2 Mathematical Model

In this paper, we consider a roundabout joining three roads as illustrated in Figure 1, the generalization of the study to an arbitrary number of roads being straightforward.

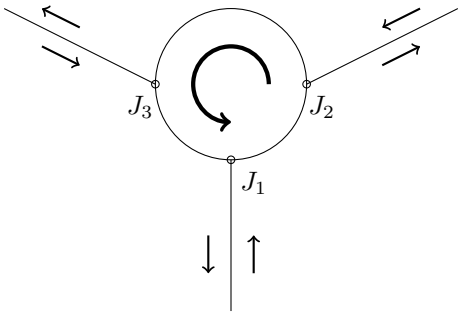

Figure 1: Sketch of the roundabout considered in the article.

A roundabout can be seen as a periodic sequence of junctions and it can be represented by an oriented graph, in which roads are described by arcs and junctions by vertexes. Each link forming the roudabout is modeled by an interval $\mathcal{I}_i = [a_i, b_i] \subset \mathbb{R}$, $i = 1, 2, 3$, $a_i < b_i$. In particular, in our case, each junction can be modeled as a 2×2 junction, see Figure 2. To recover the behavior of the roundabout, periodic

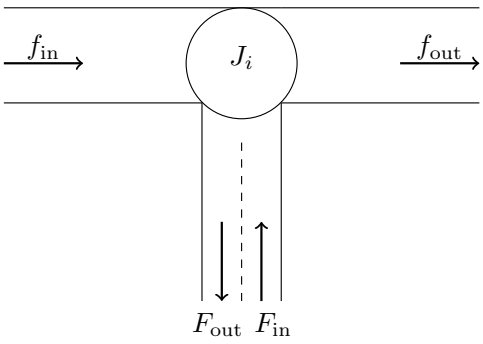

(a) Part of the roundabout.

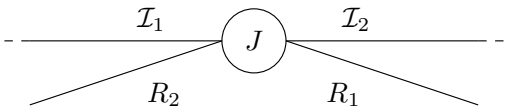

(b) Corresponded junction.

Figure 2: Detail of the network modeled in the article

boundary conditions are introduced on the main lane such that $b_i = a_{i+1}$, $i = 1, 2, 3$ and $b_3 = a_1$. At each junction we will consider the model introduced in [5], suitably modified to adapt it to the roundabout structure. The evolution of the traffic flow in the main lane segments is described by a scalar hyperbolic conservation law:

$$\partial_t \rho_i + \partial_x f(\rho_i) = 0, \quad (t, x) \in \mathbb{R}^+ \times \mathcal{I}_i \quad i = 1, 2, 3, \tag{1}$$

where $\rho_i = \rho_i(t, x) \in [0, \rho_{\max}]$ is the mean traffic density, $\rho_{\max}$ the maximal density allowed on the road and the flux function $f : [0, \rho_{\max}] \to \mathbb{R}^+$ is given by following flux-density relation:

$$f(\rho) = \begin{cases} \rho v_{\text{f}} & \text{if } 0 \le \rho \le \rho_{\text{c}}, \\ \dfrac{f^{\max}}{\rho_{\max} - \rho_c}(\rho_{\max} - \rho) & \text{if } \rho_{\text{c}} \le \rho \le \rho_{\max}, \end{cases}$$

with v_{f} the maximal speed of the traffic, $\rho_{\text{c}} = \dfrac{f^{\max}}{v_{\text{f}}}$ the critical density and $f^{\max} = f(\rho_{\text{c}})$ the maximal flux value, see Figure 3. Throughout the paper, for simplicity, we will assume $\rho_{\max} = 1$ and $v_{\text{f}} = 1$. Figure 3 gives an example of flux function satisfying the previous hypotheses.

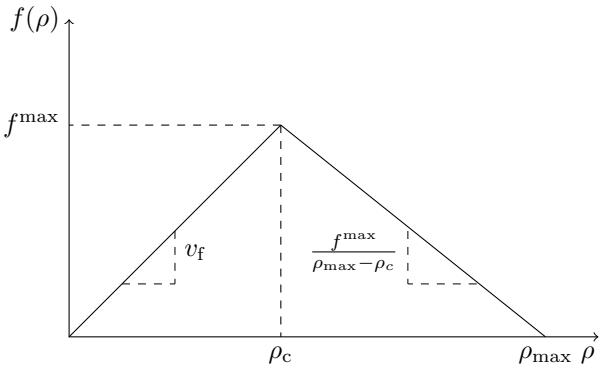

Figure 3: Flux function considered.

The incoming lanes of the secondary roads entering the junctions are modeled with a buffer of infinite size and capacity. This choice is made to avoid backward moving shocks at the boundary, for details see [5]. In particular, the evolution of the queue length of each buffer is described by an ODE:

$$\frac{dl_i(t)}{dt} = F^i_{\mathrm{in}}(t) - \gamma_{\mathrm{r1},i}(t), \quad t \in \mathbb{R}^+ \quad i = 1,2,3, \tag{2}$$

where $l_i(t) \in [0, +\infty[$ is the queue length, $F^i_{\mathrm{in}}(t)$ the flux entering the lane and $\gamma_{\mathrm{r1},i}(t)$ the flux exiting the lane into the roundabout. For simplicity, the outgoing lane is considered as a sink that accepts all the flux coming from the main lane. Moreover, no flux from the incoming lane is allowed on the outgoing stretch of the same road.
The Cauchy problem to solve is then:

$$\begin{cases} \partial_t \rho_i + \partial_x f(\rho_i) = 0, & (t,x) \in \mathbb{R}^+ \times \mathcal{I}_i, \\ \dfrac{dl_i(t)}{dt} = F^i_{\mathrm{in}}(t) - \gamma_{\mathrm{r1},i}(t), & t \in \mathbb{R}^+, \\ \rho_i(0,x) = \rho_{i,0}(x), & \text{on } \mathcal{I}_i, \\ l_i(0) = l_{i,0} \end{cases} \tag{3}$$

for $i = 1,2,3$, where $\rho_{i,0}(x)$ are the initial traffic densities and $l_{i,0}$ the initial lengths of the buffers. This will be coupled with an optimization problem at the junctions that gives the distribution of traffic among the roads.
We define the demand $d(F^i_{\mathrm{in}}, l_i)$ of the incoming lane for the secondary roads, the demand function $\delta(\rho_i)$ on the incoming main lane segment, and the supply function $\sigma(\rho_i)$ on the outgoing main lane segment at each junction as follows.

$$d(F^i_{\mathrm{in}}, l_i) = \begin{cases} \gamma^{\max}_{\mathrm{r1},i} & \text{if } l_i(t) > 0, \\ \min\left(F^i_{\mathrm{in}}(t), \gamma^{\max}_{\mathrm{r1},i}\right) & \text{if } l_i(t) = 0, \end{cases} \tag{4}$$

$$\delta(\rho_i) = \begin{cases} f(\rho_i) & \text{if } 0 \le \rho_i < \rho_{\mathrm{c}}, \\ f^{\max} & \text{if } \rho_{\mathrm{c}} \le \rho_i \le 1, \end{cases} \tag{5}$$

$$\sigma(\rho_i) = \begin{cases} f^{\max} & \text{if } 0 \le \rho_i \le \rho_{\mathrm{c}}, \\ f(\rho_i) & \text{if } \rho_{\mathrm{c}} < \rho_i \le 1, \end{cases} \tag{6}$$

for $i = 1,2,3$, where $\gamma^{\max}_{\mathrm{r1},i}$ is the maximal flow on the incoming lane $R_{1,i}$. Moreover, we introduce $\beta \in [0,1]$ the split ratio of the outgoing lane $R_{2,i}$, and its flux $\gamma_{\mathrm{r2},i}(t) = \beta f(\rho_i(t,0-))$, $i = 1,2,3$.
For simplicity, in the following of the article, we will focus on each single junction and drop the index i when not necessary.

Definition 1 *Consider a roundabout with three roads $\mathcal{I}_i = [a_i, b_i] \subset \mathbb{R}$, $a_i < b_i$, for $i = 1,2,3$, with $b_3 = a_1$, three entrances $R_{1,i}$ $i = 1,2,3$, and three exits $R_{2,i}$ $i = 1,2,3$. A collection of functions $(\rho_i, l_i)_{i=1,2,3} \in \prod_{i=1}^{3} \mathcal{C}^0\left(\mathbb{R}^+; \mathbf{L^1} \cap BV(\mathcal{I}_i)\right) \times \prod_{i=1}^{3} \mathbf{W^{1,\infty}}(\mathbb{R}^+; \mathbb{R}^+)$ is an admissible solution to (3) if*

1. *ρ_i is a weak solutions on $\mathcal{I}_i$, i.e., $\rho_i : [0, +\infty[\times\mathcal{I}_i \to [0,1]$, such that*

$$\int_{\mathbb{R}^+}\int_{\mathcal{I}_i}\Big(\rho_i\partial_t\varphi_i + f(\rho_i)\partial_x\varphi_i\Big)dxdt = 0, \tag{7}$$

for every $\varphi_i \in \mathcal{C}^1_c(\mathbb{R}^+ \times \mathcal{I}_i)$, $i = 1,2,3$.

2. *ρ_i satisfies the Kružhkov entropy condition [13] on $(\mathbb{R}\times\mathcal{I}_i)$, i.e.,*

$$\int_{\mathbb{R}^+}\int_{\mathcal{I}_i}(|\rho_i - k|\partial_t\varphi_i + \operatorname{sgn}(\rho_i - k)(f(\rho_i) - f(k))\partial_x\varphi_i)dxdt + \int_{\mathcal{I}_i}|\rho_{i,0} - k|\varphi_i(0,x)dx \geq 0 \tag{8}$$

for every $k \in [0,1]$ and for all $\varphi_i \in \mathcal{C}^1_c(\mathbb{R}\times\mathcal{I}_i)$, $i = 1,2,3$.

3. *At each junction J_i, $f(\rho_i(t,0-)) + \gamma_{\mathrm{r}1,i}(t) = f(\rho_{i+1}(t,0+)) + \gamma_{\mathrm{r}2,i}(t)$ for $i = 1,2,3$ (where we set $\rho_4 = \rho_1$).*

4. *At each junction J_i, the flux of the outgoing main lane $f(\rho_{i+1}(t,0+))$ is maximum subject to*

$$f(\rho_{i+1}(t,0+)) = \min\Big((1-\beta)\delta(\rho_i(t,0-)) + d(F_{\mathrm{in}}(t), l_i(t)), \sigma(\rho_{i+1}(t,0+))\Big), \tag{9}$$

for $i = 1,2,3$, and $\rho_4 = \rho_1$ and 3.

5. *l_i is a solution of (2) for almost every $t \in \mathbb{R}^+$, $i = 1,2,3$.*

Remark 1 *A parameter $P \in]0,1[$ is introduced to ensure uniqueness of the solution. More precisely, P is a right of way parameter that defines the amount of flux that enters the outgoing main lane from each incoming road. When the priority applies, $Pf(\rho_i(t,0+))$ is the flux allowed from the incoming main lane into the outgoing main lane, and $(1-P)f(\rho_{i+1}(t,0+))$ the flux from the entrance of the roundabout.*

3 Riemann Problem at the junction

In this section we describe the construction of the Riemann Solver at a junction and then we apply it to our particular case to recover the expressions of the cost functionals. The Riemann problem at J is the Cauchy problem (3) where the initial conditions are given by $\rho_{0,i}(x) \equiv \rho_{0,i}$ on $\mathcal{I}_i$ for $i = 1,2,3$. In the following, we will focus only on one junction J with two incoming roads and two outgoing ones. We fix constants $\rho_{1,0}, \rho_{2,0} \in [0,1]$, $l_0 \in [0,+\infty[$, $F_{\mathrm{in}} \in]0,+\infty[$ and a priority factor $P \in]0,1[$. We define the Riemann Solver at junction by means of a Riemann Solver $\mathcal{RS}_{\bar{l}} : [0,1]^2 \to [0,1]^2$, which depends on the instantaneous load of the buffer $\bar{l}$. For each $\bar{l}$ the Riemann Solver $\mathcal{RS}_{\bar{l}}(\rho_{1,0},\rho_{2,0}) = (\hat{\rho}_1, \hat{\rho}_2)$ is constructed in the following way.

1. Define $\Gamma_1 = f(\rho_1(t,0-))$, $\Gamma_2 = f(\rho_2(t,0+))$, $\Gamma_{\mathrm{r}1} = \gamma_{\mathrm{r}1}(t)$;
2. Consider the space $(\Gamma_1, \Gamma_{\mathrm{r}1})$ and the sets $\mathcal{O}_1 = [0, \delta(\rho_{1,0})]$, $\mathcal{O}_{\mathrm{r}1} = [0, d(F_{\mathrm{in}}, \bar{l})]$;
3. Trace the lines $(1-\beta)\Gamma_1 + \Gamma_{\mathrm{r}1} = \Gamma_2$; and $\Gamma_1 = \frac{P}{(1-P)(1-\beta)}\Gamma_{\mathrm{r}1}$;
4. Consider the region

$$\Omega = \Big\{(\Gamma_1, \Gamma_{\mathrm{r}1}) \in \mathcal{O}_1 \times \mathcal{O}_{\mathrm{r}1} : (1-\beta)\Gamma_1 + \Gamma_{\mathrm{r}1} \in [0, \Gamma_2]\Big\}. \tag{10}$$

Different situations can occur depending on the value of Γ_2:

- Demand-limited case: Γ_2=$(1-\beta)\delta(\rho_{1,0}) + d(F_{\mathrm{in}}, \bar{l})$.
  We set $\hat{\Gamma}_1 = \delta(\rho_{1,0})$, $\hat{\Gamma}_{\mathrm{r}1} = d(F_{\mathrm{in}}, \bar{l})$ and $\hat{\Gamma}_2 = (1-\beta)\delta(\rho_{1,0}) + d(F_{\mathrm{in}}, \bar{l})$, as illustrated in Figure 4(a).

- Supply-limited case: $\Gamma_2 = \sigma(\rho_{2,0})$.
  We set Q to be the point of intersection of $(1-\beta)\Gamma_1 + \Gamma_{r1} = \Gamma_2$ and $\Gamma_1 = \frac{P}{(1-P)(1-\beta)}\Gamma_{r1}$. If $Q \in \Omega$, we set $(\hat{\Gamma}_1,\hat{\Gamma}_{r1})=Q$ and $\hat{\Gamma}_2 = \Gamma_2$, see Figure 4(b); if $Q \notin \Omega$, we set $(\hat{\Gamma}_1,\hat{\Gamma}_{r1})=S$ and $\hat{\Gamma}_2 = \Gamma_2$, where S is the point of the segment $\Omega \cap (\Gamma_1, \Gamma_{r1}) : (1-\beta)\Gamma_1 + \Gamma_{r1} = \Gamma_2$ closest to the line $\Gamma_1 = \frac{P}{(1-P)(1-\beta)}\Gamma_{r1}$ see Figure 4(c).

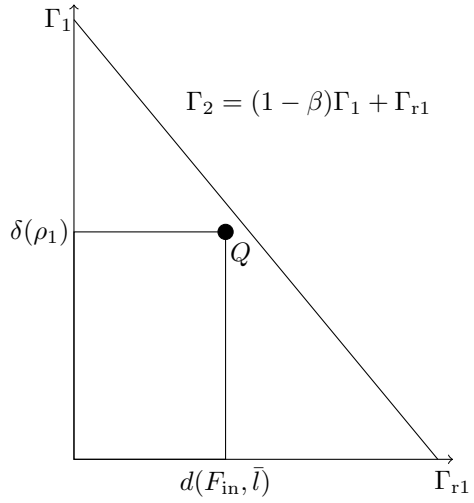

(a) Demand-limited case

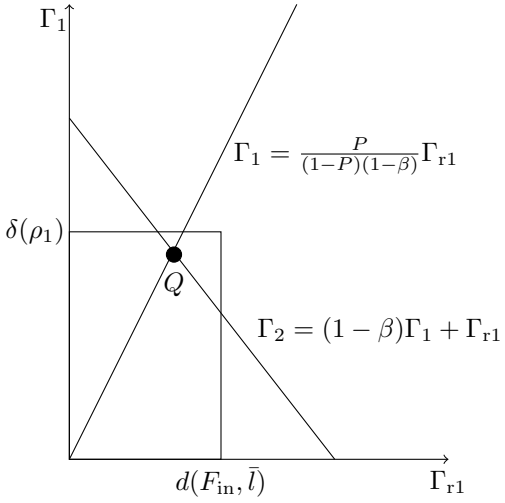

(b) Supply-limited case: intersection inside Ω

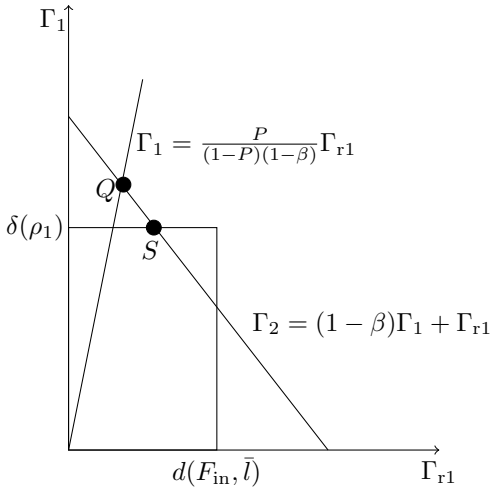

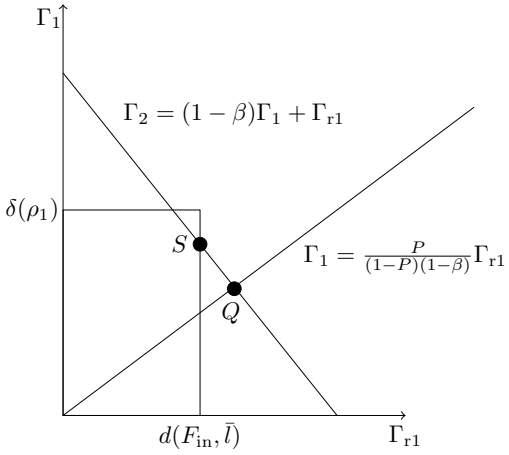

(c) Supply-limited case: intersection outside Ω

Figure 4: Solutions of the Riemann Solver at the junction.

Also, we define the function τ as follows, for details see [14].

Definition 2 *Let $\tau : [0,1] \to [0,1]$ be the map such that:*

- *$f(\tau(\rho)) = f(\rho)$ for every $\rho \in [0,1]$;*
- *$\tau(\rho) \neq \rho$ for every $\rho \in [0,1] \setminus \{\rho_c\}$.*

Remark 2 *Compared to [5], the model presented in this paper has a modified Riemann Problem at junction. In particular, on roundabouts exits precede entrances. Therefore, the flow coming from the main lane and crossing the junction, interacting with the incoming flow, is $(1-\beta)\Gamma_1$. This leads to*

consider the priority line as $\Gamma_1 = \frac{P}{(1-P)(1-\beta)}\Gamma_{r1}$ *adding a factor of* $\frac{1}{1-\beta}$ *with respect to the other model. This takes into account the amount of people that leave the roundabout before the entrance. All the proofs in [5] can be extended and adapted to fit this case.*

The following result holds, see [5, Theorem 3.2]

Theorem 1 *Consider a junction* J *and fix a right f way parameter* $P \in]0,1[$*. For every* $\rho_{1,0}, \rho_{2,0} \in [0,1]$ *and* $l_0 \in [0, +\infty[$ *there exists a unique admissible solution* $(\rho_1(t,x), \rho_2(t,x), l(t))$ *in the sense of Definition 1, compatible with the Riemann Solver proposed in Section 3. More precisely, there exists a unique couple* $(\hat{\rho}_1, \hat{\rho}_2) \in [0,1]^2$ *such that* $\mathcal{RS}_{\bar{l}}(\rho_{1,0}, \rho_{2,0}) = (\hat{\rho}_1, \hat{\rho}_2)$*:*

$$\hat{\rho}_1 \in \begin{cases} \{\rho_{1,0}\} \cup]\tau(\rho_{1,0}), 1] & \text{if } 0 \le \rho_{1,0} \le \rho_c, \\ [\rho_c, 1] & \text{if } \rho_c \le \rho_{1,0} \le 1, \end{cases} \qquad f(\hat{\rho}_1) = \hat{\Gamma}_1, \tag{11}$$

and

$$\hat{\rho}_2 \in \begin{cases} [0, \rho_c] & \text{if } 0 \le \rho_{2,0} \le \rho_c, \\ \{\rho_{2,0}\} \cup [0, \tau(\rho_{2,0})[& \text{if } \rho_c \le \rho_{1,0} \le 1, \end{cases} \qquad f(\hat{\rho}_2) = \hat{\Gamma}_2. \tag{12}$$

For the incoming road the solution is given by the wave $(\rho_{1,0}, \hat{\rho}_1)$*, while for the outgoing road the solution is given by the wave* $(\hat{\rho}_2, \rho_{2,0})$*. Furthermore, for a.e.* $t > 0$*, it holds*

$$(\rho_1(t,0-), \rho_2(t,0+)) = \mathcal{RS}_{l(t)}(\rho_1(t,0-), \rho_2(t,0+)).$$

For the proof, see [5].

4 Optimization on networks

In this section we define the optimization problem, the cost functionals and derive their expressions. We introduce the Total Travel Time (TTT) on the road network and the Total Waiting Time (TWT) on the incoming lanes of the secondary roads, which are defined as follows:

$$TTT(T, \vec{P}) = \sum_{i=1}^{3} \int_0^T \int_{\mathcal{I}_i} \rho(t,x)dxdt + \sum_{i=1}^{3} \int_0^T l_i(t)dt + T \cdot \sum_{i=1}^{3} \int_{\mathcal{I}_i} \rho(T,x)dx + T \cdot \sum_{i=1}^{3} l_i(T) \tag{13}$$

$$TWT(T, \vec{P}) = \sum_{i=1}^{3} \int_0^T l_i(t)dt + T \cdot l_i(T) \tag{14}$$

for $T > 0$ that we will take sufficiently large so that the solution is stabilized. Our aim is to minimize (13), (14) with respect to the right of way parameter P. To this end, we derive the explicit expression of the cost functionals locally at junctions to study their dependence on the right of way parameter P. We consider a single junction as in Figure 2(b) with $\mathcal{I}_1 = [-1, 0]$ and $\mathcal{I}_2 = [0, 1]$. We suppose that the network and the buffer are empty at $t = 0$ and we assume that the following boundary data are given: f^{in} the inflow on the incoming main lane, f^{out} the outflow on the outgoing main lane and F_{in} the incoming flux of the secondary road. Moreover, to reduce the number of cases to be studied, we assume $F_{\text{in}} \le f^{\max} = \gamma_{r1}^{\max}$ and $f^{\text{out}} \le f^{\max}$. Now, we can solve the corresponding initial-boundary value problem.
The first step is to compute the demand and supply functions of the roads. We have $\delta(\rho_{1,0}) = 0$, $d(F_{\text{in}}, l) = \min(F_{\text{in}}, \gamma_{r1}^{\max}) = F_{\text{in}}$ and $\sigma(\rho_{2,0}) = f^{\max}$. Then we can compute Γ_2:

$$\Gamma_2 = \min\Big((1-\beta)\delta(\rho_{1,0}) + d(F_{\text{in}}, l), \sigma(\rho_{2,0})\Big) = F_{\text{in}}.$$

It is straightforward to see that the problem is demand limited, hence the optimal point is the point at maximal demands. Thus it follows $\hat{\Gamma}_1 = 0$, $\hat{\Gamma}_2 = F_{\text{in}}$ and $\hat{\Gamma}_{r1} = F_{\text{in}}$, from which we derive $\hat{\rho}_1 = \rho_{1,0} = 0$ and $\hat{\rho}_2 = F_{\text{in}} < \rho_c$. Since we are demand limited we also have $l(t) = 0$. The solution in the $x - t$ plane looks as in Figure 5. The wave produced by the junction problem interacts with the right boundary $x = 1$ at time $t_1 = 1$. Moreover at $x = -1$, the boundary condition enforces the creation of an additional

wave at $t = 0$ with speed equal to 1. This gives a density $\hat{\rho}_1 = f^{\text{in}} < \rho_c$, which reaches the junction at the same time $t_1 = 1$, see Figure 5.

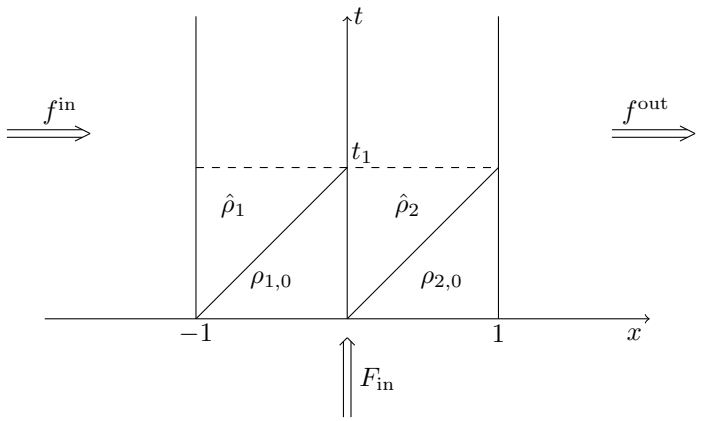

Figure 5: Solution of the initial-boundary value problem for $t \in [0, t_1]$.

At $t_1 = 1$ we solve a new Riemann problem at the junction with initial densities

$$\rho(1, x) = \begin{cases} \hat{\rho}_1 & \text{if } x < 0, \\ \hat{\rho}_2 & \text{if } x > 0. \end{cases}$$

We assume that the splitting ratio $\beta \in (0, 1)$ is the same for all roads and fixed. The demand and supply functions on the respective roads are $\delta(\hat{\rho}_1) = f^{\text{in}}$, $d(F_{\text{in}}, l_0) = \min(F_{\text{in}}, \gamma_{\text{r1}}^{\max}) = F_{\text{in}}$, $\sigma(\hat{\rho}_2) = f^{\max}$. Computing Γ_2 from these values we obtain

$$\Gamma_2 = \min\Big((1-\beta)\delta(\hat{\rho}_1) + d(F_{\text{in}}, l), \sigma(\hat{\rho}_2)\Big)$$

Two cases can occur at this point according to the value of Γ_2:

4.1 $\Gamma_2 = (1-\beta)\delta(\hat{\rho}_1) + d(F_{\text{in}}, l)$

In this case the Riemann problem at t_1 is demand limited. No wave is created in the incoming link, and a wave with speed 1 emanates from the junction on the outgoing road with a density $\rho_2 = (1-\beta)f^{\text{in}} + F_{\text{in}}$. The buffer remains empty. At this point we have two different situations according to:

- $F_{\text{in}} < f^{\text{out}}$,
- $f^{\text{out}} < F_{\text{in}}$.

In the first case ($F_{\text{in}} < f^{\text{out}}$) the wave from the junction interacts with the boundary $x = 1$ at $t_2 = 2$, generating a wave with negative speed and a density $\rho_3 = \dfrac{f^{\max} - (1-f^{\max})f^{\text{out}}}{f^{\max}} \in [\rho_c, 1]$ which reaches the junction at $t_3 = \dfrac{2\lambda(\rho_2, \rho_3) - 1}{\lambda(\rho_2, \rho_3)}$ as shown in Figure 6.

Above $\lambda(\rho_2, \rho_3) = \dfrac{((1-\beta)f^{\text{in}} + F_{\text{in}} - f^{\text{out}})f^{\max}}{(1-\beta)f^{\text{in}}f^{\max} + F_{\text{in}}f^{\max} - f^{\max} + (1-f^{\max})f^{\text{out}}}$ is given by the Rankine-Hugoniot jump condition.

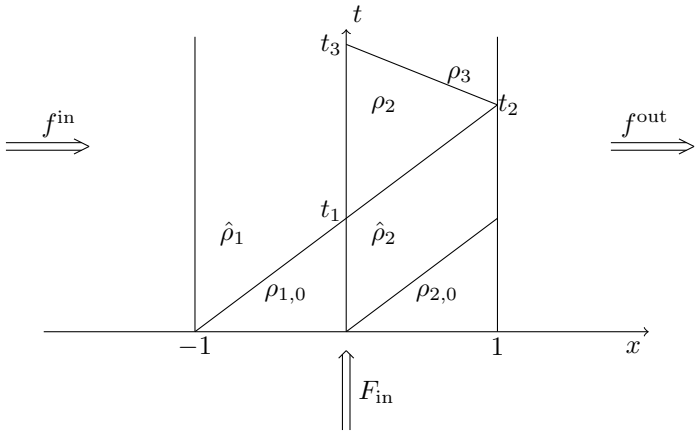

Figure 6: Solution of the junction problem for $t \in [0, t_3]$

In the second case ($f^{\text{out}} < F_{\text{in}}$) at time t_1 the wave that interacts with the boundary $x = 1$ produces a wave with negative speed and the same density ρ_3 as above. This wave intersect the wave that comes out from the junction at time t_1 generating an additional wave with negative speed. At the point of intersection (t_o, x_o) a new Riemann problem needs to be solved, which creates another wave which reaches the junction at time $t_3 = t_o - \dfrac{1}{\lambda(\rho_2, \rho_3)}$ as shown in Figure 7.

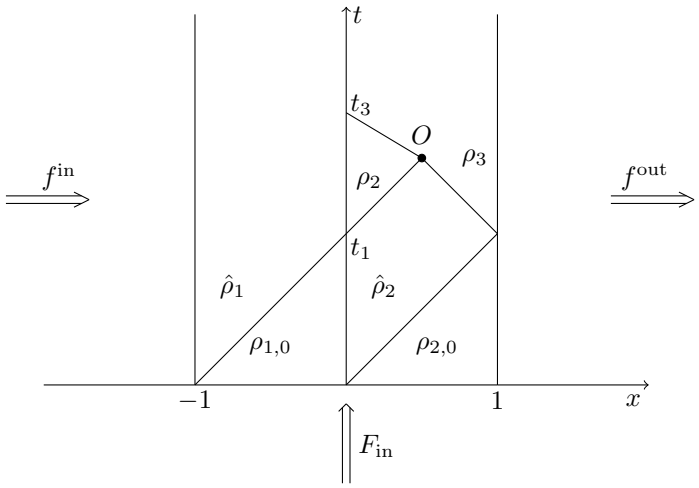

Figure 7: Solution of the junction problem for $t \in [0, t_3]$

In both cases at t_3

$$f^{\text{out}} \leq (1-\beta) f^{\text{in}} + F_{\text{in}}.$$

Clearly, at time t_3 the junction problem is supply limited resulting in the following fluxes $\Gamma_2 = f^{\text{out}}$, $\Gamma_1 = \dfrac{P}{1-\beta} f^{\text{out}}$ and $\Gamma_{\text{r1}} = (1-P) f^{\text{out}}$. Moreover, let us introduce the following values

- $P_1 = \dfrac{f^{\text{out}} - F_{\text{in}}}{f^{\text{out}}}$,
- $P_2 = \dfrac{(1-\beta) f^{\text{in}}}{f^{\text{out}}}$.

Observe that

$$P_2 - P_1 = \frac{(1-\beta) f^{\text{in}}}{f^{\text{out}}} - \frac{f^{\text{out}} - F_{\text{in}}}{f^{\text{out}}} = \frac{(1-\beta) f^{\text{in}} + F_{\text{in}} - f^{\text{out}}}{f^{\text{out}}} \geq 0, \tag{15}$$

which implies $P_1 \leq P_2$, see Figure 8

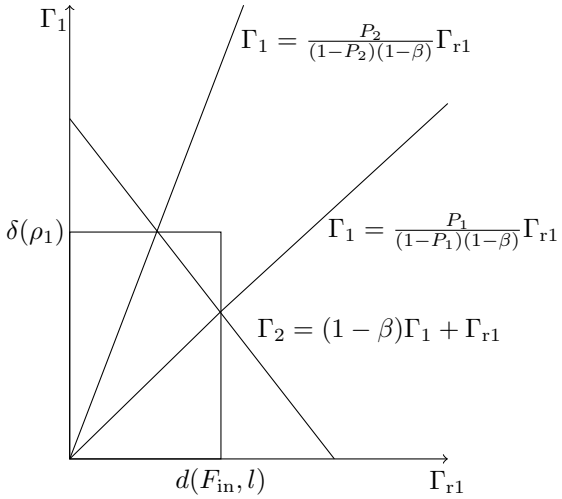

Figure 8: Relationship between P_1 and P_2

The solutions of the Riemann problem at the junction are given by:

(1a) If $\max(0, P_1) \leq P \leq \min(P_2, 1)$, then $\left(\frac{P}{1-\beta} f^{\text{out}}, (1-P) f^{\text{out}}, f^{\text{out}}\right)$ is the solution of Riemann problem.

(2a) If $1 \geq P > \min(P_2, 1)$, then $\left(f^{\text{in}}, f^{\text{out}} - (1-\beta) f^{\text{in}}, f^{\text{out}}\right)$ is the solution.

(3a) If $0 \leq P < \max(0, P_1)$, then $\left(\frac{f^{\text{out}} - F_{\text{in}}}{1-\beta}, F_{\text{in}}, f^{\text{out}}\right)$ is the solution.

According to the different values of P, different cases can occur. For this reason we only sketch the computation of the cost functionals. We refer the reader to [15] for the details.

4.1.1 Case $\max(0, P_1) \leq P \leq \min(P_2, 1)$.

We solve the Riemann problem at t_3. The solution of the Riemann Problem is given by (1a). From this it follows

$$\rho_1 = \frac{(1-\beta) f^{\max} - (1 - f^{\max}) P f^{\text{out}}}{(1-\beta) f^{\max}} \tag{16}$$

and the wave speed $\lambda(\hat{\rho}_1, \rho_1)$ is

$$\lambda(\hat{\rho}_1, \rho_1) = \frac{\left(f^{\text{in}}(1-\beta) - P f^{\text{out}}\right) f^{\max}}{(1-\beta)(f^{\text{in}} - 1) f^{\max} + (1 - f^{\max}) P f^{\text{out}}} \tag{17}$$

The characteristic $x = \lambda(\hat{\rho}_1, \rho_1)(t - t_3)$ crosses the boundary $x = -1$ at

$$t_4 = t_3 - \frac{1}{\lambda(\hat{\rho}_1, \rho_1)} \tag{18}$$

On the outgoing road there is no new wave created since $\hat{\Gamma}_2 = f^{\text{out}} = f(\rho_3)$ which can be seen in Figure 9.

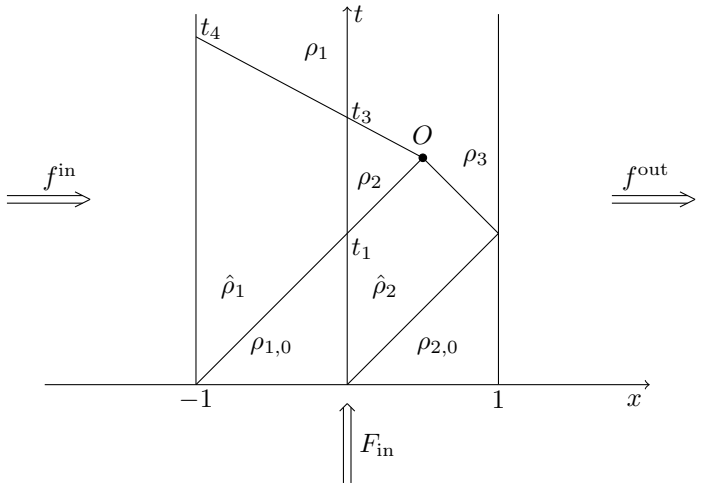

Figure 9: Solution for $t \in [0, t_4]$.

The buffer length is given by

$$l(t) = (F_{\text{in}} - (1-P)f^{\text{out}})(t - t_3) > 0, \quad \text{for } t > t_3. \tag{19}$$

4.1.2 Case $\min(P_2, 1) < P \leq 1$.

In this case the solution of the Riemann Problem is given by (2a). On the incoming main road there is no wave with negative speed exiting the junction. Similarly, on the outgoing main road there is no wave since $\hat{\Gamma}_2 = f^{\text{out}}$. The solution is shown in Figure 10. The buffer increases since $l(t) = (F_{\text{in}} + (1-\beta)f^{\text{in}} - f^{\text{out}})(t - t_3) > 0$.

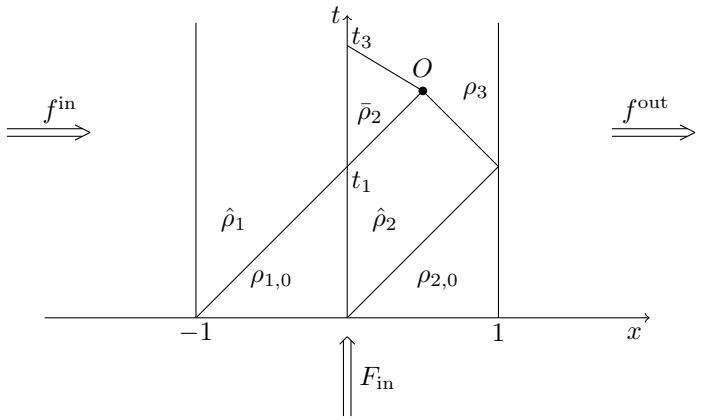

Figure 10: Solution for $t \in [0, t_3]$ in the case $\min(P_2, 1) \leq P < 1$.

4.1.3 Case $0 \leq P < \max(0, P_1)$.

The solution of the Riemann problem is given by (3a). We get

$$\check{\rho}_1 = \frac{f^{\max}(1 - \beta + f^{\text{out}} - F_{\text{in}}) + F_{\text{in}} - f^{\text{out}}}{(1-\beta)f^{\max}}. \tag{20}$$

The wave with characteristic speed

$$\lambda(\hat{\rho}_1, \check{\rho}_1) = \frac{f^{\text{in}} - \hat{\Gamma}_1}{\hat{\rho}_1 - \check{\rho}_1} = \frac{\Big((1-\beta)f^{\text{in}} + F_{\text{in}} - f^{\text{out}}\Big)f^{\max}}{(1-\beta)f^{\text{in}}f^{\max} - f^{\max}(1 - \beta + f^{\text{out}} - F_{\text{in}}) + F_{\text{in}} - f^{\text{out}}} \tag{21}$$

emanating from the junction crosses the boundary $x = -1$ at time $t = t_4$ expressed as:

$$t_4 = t_3 - \frac{1}{\lambda(\hat{\rho}_1, \check{\rho}_1)} \tag{22}$$

Since $\dfrac{f^{\text{out}} - F_{\text{in}}}{1-\beta} < \delta(\hat{\rho}_1) = f^{\text{in}}$, there is no wave produced by the interaction with the boundary $x = -1$ at time t_4. Also, on the outgoing main lane there is no new wave. The complete solution at t_4 is depicted in Figure 11.

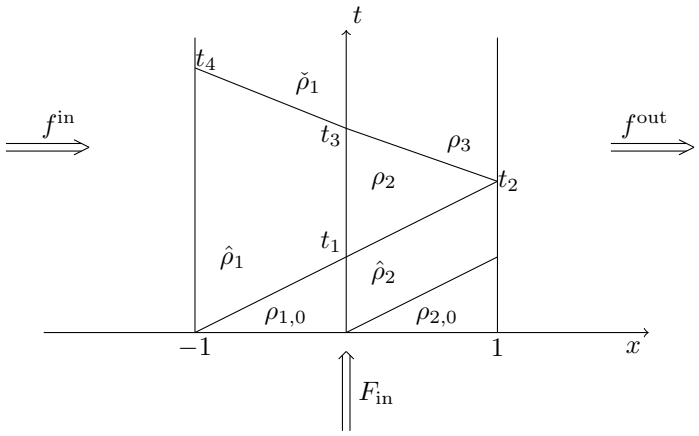

Figure 11: Complete solution for $t \in [0, t_4]$.

From the value of $\hat{\Gamma}_{r1}$ we can solve the ODE (2) and find $l(t) = 0$. This conclude the analysis of this subsection.

4.2 $\Gamma_2 = \sigma(\hat{\rho}_2)$

In this case we have

$$f^{\max} \leq (1-\beta) f^{\text{in}} + F_{\text{in}} \tag{23}$$

and hence, it is straightforward to compute the value of $\Gamma_2 = f^{\max}$, $\Gamma_1 = \dfrac{P}{1-\beta} f^{\max}$ and $\Gamma_{\text{r1}} = (1-P) f^{\max}$.
Moreover, let us introduce

- $P_1 = \dfrac{f^{\max} - F_{\text{in}}}{f^{\max}}$,
- $P_2 = \dfrac{(1-\beta) f^{\text{in}}}{f^{\max}}$.

Observe that also in this case it holds

$$P_2 - P_1 = \frac{(1-\beta) f^{\text{in}}}{f^{\max}} - \frac{f^{\max} - F_{\text{in}}}{f^{\max}} = \frac{(1-\beta) f^{\text{in}} + F_{\text{in}} - f^{\max}}{f^{\max}} \geq 0 \tag{24}$$

because of (23), which implies $P_1 \leq P_2$, see Figure 12. Then the solutions of the Riemann problem at the junction are given by

(1b) If $P_1 \leq P \leq P_2$, then $\left(\dfrac{P}{1-\beta} f^{\max}, (1-P) f^{\max}, f^{\max} \right)$ is the solution of Riemann problem.

(2b) If $P \geq P_2$, then $\left(f^{\text{in}}, f^{\max} - (1-\beta) f^{\text{in}}, f^{\max} \right)$ is the solution.

(3b) If $P \leq P_1$, then $\left(\dfrac{f^{\max} - F_{\text{in}}}{1-\beta}, F_{\text{in}}, f^{\max} \right)$ is the solution.

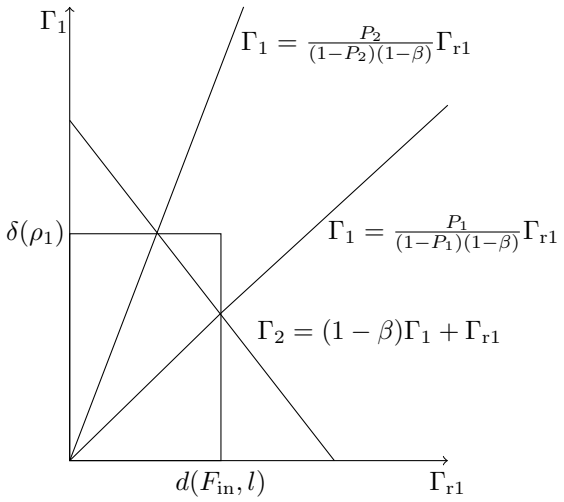

Figure 12: Relationship between P_1 and P_2

According to the different values of P different cases can occur. We only sketch the computation of the cost functionals. We refer the reader to [15] for the details.

4.2.1 Case $P_1 \leq P \leq P_2$.

In this case, at time t_1 the interaction between the wave in the outgoing road and the boundary at $x = 1$ can generate an additional wave if $F_{in} > f^{out}$. When this is the case, in fact, there is a wave with negative speed which can interact with other waves between $[0, 1]$. We make the following assumption:

$$F_{in} > f^{out}. \tag{25}$$

In this case, depending on the priority parameter P, the waves emanating from the junction at t_1 and t_4 can collide within the region $-1 < x < 0$. This, in particular, occurs for the value of the priority parameter $P = \bar{P}$, given by

$$\bar{P} = \frac{(1-\beta)\Big((f^{max})^2 + f^{max}(2f^{in} - f^{out} - f^{in}F_{in} + f^{out}f^{in}) + 2f^{out}f^{in}\Big)}{f^{max}(F_{in}f^{max} - f^{max} + f^{out} - f^{out}f^{max})} \tag{26}$$

where $\bar{P}$ is the value at which the waves interact at $x = -1$. We can, then, distinguish two additional cases $P_1 \leq P < \bar{P}$ and $\bar{P} \leq P \leq P_2$.

1. $P_1 \leq P < \bar{P}$. In this case, the waves do not interact in the region $-1 < x < 0$ and no new waves are created. Hence, the study is concluded and the solution is depicted in Figure 13.
2. $\bar{P} \leq P \leq P_2$. In this case there is a collision between the waves emanating from the junction at t_1 and t_4 on the incoming link and the final solution is showed in Figure 14.

For all cases for $t \geq t_4$ the buffer length increases linearly with a value

$$l(t) = l(t_4) + \big(F_{in} - (1-P)f^{out}\big)(t - t_4) > 0. \tag{27}$$

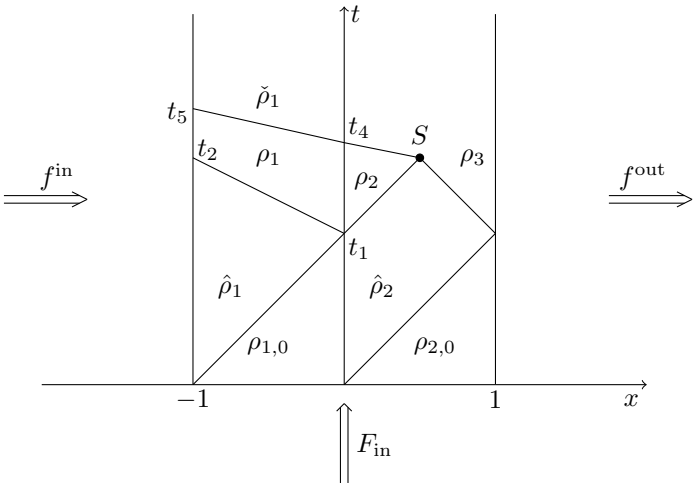

Figure 13: Solution of the problem in $[0, t_5]$

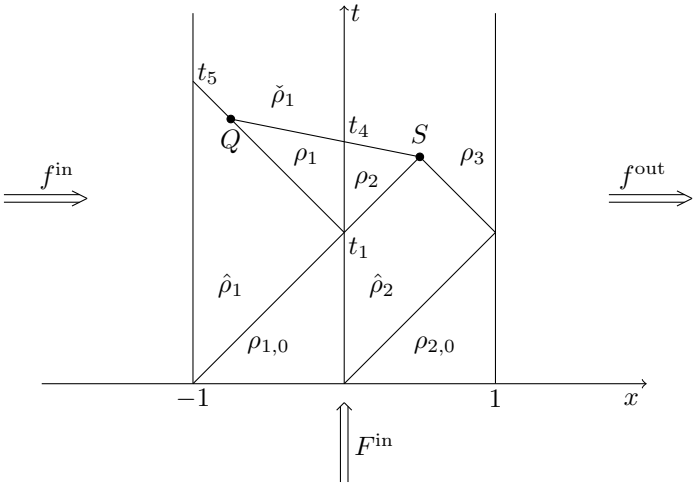

Figure 14: Solution for $t \in [0, t_5]$ with $\bar{P} \leq P \leq P_2$.

This concludes the analysis of the case $P_1 \leq P \leq P_2$.

4.2.2 Case $P > P_2$.

The solution of the Riemann problem is given by (2b). In this case, $\rho_1 = \hat{\rho}_1$ and no wave is created in the incoming main lane. On the outgoing link we have $\rho_2 = \rho_c$, which generates a wave with speed equal to 1. The buffer length increases since $l(t) = (F_{\text{in}} + (1-\beta)f^{\text{in}} - f^{\max})(t-1) > 0$. The wave with positive speed 1 generated at $(t_1, 0)$ interacts with the wave generated from right boundary at point $S = (t_S, x_S)$ at time $t = t_S$ under assumption (25), see Figure 15. At the right boundary $f^{out} = \dfrac{1-\rho_3}{1-f^{max}} f^{max}$, hence we obtain that

$$\rho_3 = 1 - \frac{f^{\text{out}}(1 - f^{\max})}{f^{\max}}. \tag{28}$$

At t_4 the Riemann problem at the junction to solve is then

$$\rho(t_4, x) = \begin{cases} \hat{\rho}_1 & \text{if } x < 0, \\ \rho_3 & \text{if } x > 0, \end{cases}$$

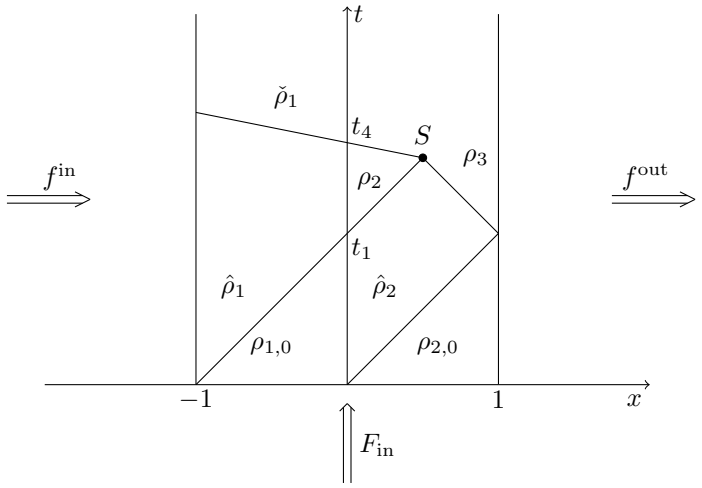

Figure 15: Solution in the case $P \geq P_2$

coupled with the following demand and supply functions

$$d(F_{\text{in}}, l) = \gamma_{\text{r1}}^{\max} = f^{\max}, \tag{29}$$

$$\delta(\hat{\rho}_1) = f^{\text{in}}, \tag{30}$$

$$\sigma(\rho_3) = f^{\text{out}}. \tag{31}$$

We can now compute

$$\Gamma_2 = \min\Big((1-\beta)\delta(\hat{\rho}_1) + d(F_{\text{in}}, l), \sigma(\rho_3)\Big) = \min\Big((1-\beta)f^{\text{in}} + f^{\max}, f^{\text{out}}\Big) = f^{\text{out}}$$

and

$$\hat{\Gamma}_1 = \frac{P}{1-\beta} f^{\text{out}}.$$

Two cases can occur at this point. If $(1-\beta)f^{\text{in}} < f^{\text{out}}$ the solution of the Riemann Problem at the junction is given by $(\hat{\Gamma}_1, \hat{\Gamma}_{\text{r1}}, \hat{\Gamma}_2) = (f^{\text{in}}, f^{\text{out}} - (1-\beta)f^{\text{in}}, f^{\text{out}})$ for all values of $P > \bar{\bar{P}} = (1-\beta)\dfrac{f^{\text{in}}}{f^{\text{out}}}$. From this it is straightforward to see that $\hat{\rho}_1 = \rho_1$ since $f^{\text{in}} = \hat{\rho}_1$ for $v_{\text{f}} = 1$. No new waves are created. For $P_2 < P < \bar{\bar{P}}$ we have $(\hat{\Gamma}_1, \hat{\Gamma}_{\text{r1}}, \hat{\Gamma}_2) = \left(\dfrac{P}{1-\beta} f^{\text{out}}, (1-P)f^{\text{out}}, f^{\text{out}}\right)$. The solution of the problem in this case is similar to the case $(1-\beta)f^{\text{in}} > f^{\text{out}}$ hence, we defer its description in the following. If $(1-\beta)f^{\text{in}} > f^{\text{out}}$ the solution of the Riemann problem at the junction becomes

$$(\hat{\Gamma}_1, \hat{\Gamma}_{\text{r1}}, \hat{\Gamma}_2) = \left(\frac{P}{1-\beta} f^{\text{out}}, (1-P)f^{\text{out}}, f^{\text{out}}\right).$$

From this we can uniquely recover the corresponding values of the densities. The solution looks as in Figure 15. The buffer increases linearly and its expression is given by

$$l(t) = l(t_4) + \left(F_{\text{in}} - (1-P)f^{\text{out}}\right)(t - t_4) > 0. \tag{32}$$

This completes the analysis for this case.

4.2.3 The case $P \leq P_1$.

The solution of the Riemann problem is given by (3b). In this case, the computations are similar to those of Section 4.2.1. The solution is sketched in Figure 16. To be noted that the point of intersection N in this case does not depend on the value of P but on the value of the other parameters.

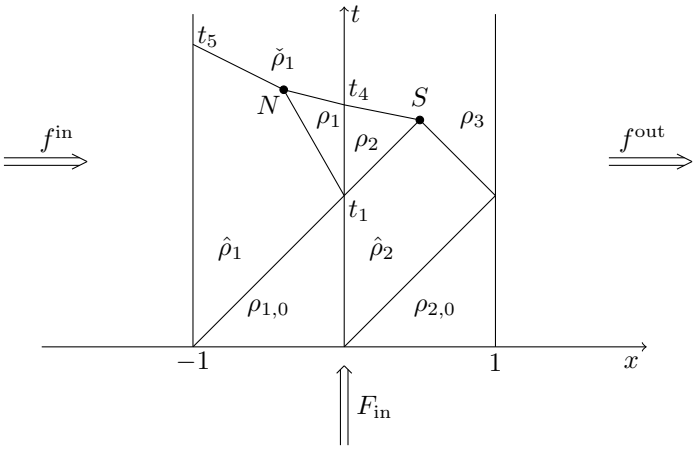

Figure 16: Solution in the case $P \leq P_1$

Finally, we compute the queue length at t_4 which is given by

$$l(t) = l(t_4) + \left(F_{\text{in}} - (1-P)f^{\text{out}}\right)(t - t_4) > 0. \tag{33}$$

4.3 Local Total Waiting Time and Total Travel Time

We are now ready to compute the expressions for the Total Travel Time and the Total Waiting Time for each value of P.
Case 4.1

- $\max(P_1, 0) \leq P \leq \min(P_2, 1)$

We calculate the TWT_{loc} as follows

$$TWT_{loc}(T, P) = \int_{t_3}^{T} (F_{\text{in}} - (1-P)f^{\text{out}})(t - t_3)dt + T(F_{\text{in}} - (1-P)f^{\text{out}})(T - t_3). \tag{34}$$

while the $TTT_{loc}(T)$ is obtained by a constant term which does not depend on P plus a term depending on the priority, that we denote by $TTT_{loc}(T, P)$:

$$\begin{aligned} TTT_{loc}(T, P) = &\iint_{A_1} \hat{\rho}_1 dtdx + \iint_{A_2} \rho_1(P)dtdx + T\int_0^1 (\rho_1(P) + \rho_3)\, dx \\ &+ \int_{t_3}^{T} (F_{\text{in}} - (1-P)f^{\text{out}})(t - t_3)dt + T(F_{\text{in}} - (1-P)f^{\text{out}})(T - t_3), \end{aligned} \tag{35}$$

where the areas of the integration domains are defined by
$A_1 = \frac{1}{2}(t_4(P) - t_3) = A_2$
as shown in Figure 17.

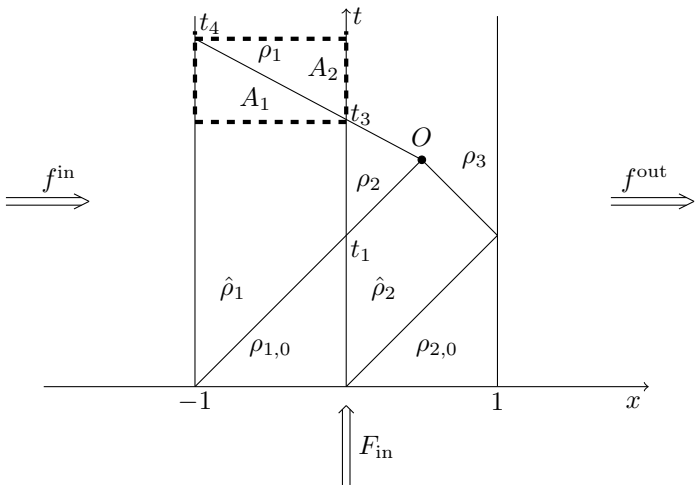

Figure 17: Area of integration in the case $P_1 \leq P \leq P_2$

- $\min(P_2, 1) < P \leq 1$

The $TWT_{loc}(T, P)$ is computed as

$$TWT_{loc}(T,P) = \int_{t_3}^{T} (F_{\text{in}} + (1-\beta)f^{\text{in}} - f^{\text{out}})(t-t_3)dt + T(F_{\text{in}} + (1-\beta)f^{\text{in}} - f^{\text{out}})(T-t_3). \quad (36)$$

The $TTT_{loc}(T)$ is given by a constant term plus

$$TTT_{loc}(T,P) = T\int_0^1 (\hat{\rho}_1 + \rho_3)\,dx + \int_{t_3}^{T} (F_{\text{in}} + (1-\beta)f^{\text{in}} - f^{\text{out}})(t-t_3)dt + T(F_{\text{in}} + (1-\beta)f^{\text{in}} - f^{\text{out}})(T-t_3). \quad (37)$$

- $0 \leq P \max(P_1, 0)$

In this case $TWT_{loc} = 0$ since the buffer is empty.
The $TTT_{loc}(T)$ is given by a constant term plus

$$TTT_{loc}(T,P) = T\int_0^1 (\check{\rho}_1 + \rho_3)\,dx. \quad (38)$$

Case 4.2

- $P_1 \leq P < \bar{P}$

We compute the TWT_{loc} as follows

$$\begin{aligned} TWT_{loc}(T,P) = &\int_{t_1}^{t_4} \left((F_{\text{in}} - (1-P)f^{\max})\,(t-1)\right) dt \\ &+ \int_{t_4}^{T} \left(l(t_4) + \left(F_{\text{in}} - (1-P)f^{\text{out}}\right)(t-t_4)\right) dt + Tl(t_4) \\ &+ T\left(F_{\text{in}} - (1-P)f^{\text{out}}\right)(T-t_4). \end{aligned} \quad (39)$$

Concerning $TTT_{loc}(T)$, it is given by a constant plus

$$\begin{aligned} TTT_{loc}(T,P) = &\int_{A_1} \hat{\rho}_1 dtdx + \int_{A_2} \rho_1(P) dtdx + \iint_{A_3} \check{\rho}_1(P) dtdx \\ &+ \int_{t_1}^{t_4} \left((F_{\text{in}} - (1-P) f^{\max}) (t-1) \right) dt \\ &+ \int_{t_4}^{T} \left(l(t_4) + \left(F_{\text{in}} - (1-P) f^{\text{out}} \right) (t-t_4) \right) dt \\ &+ T l(t_4) + T \left(F_{\text{in}} - (1-P) f^{\text{out}} \right) (T-t_4) + T \int_0^1 \left(\check{\rho}_1(P) + \rho_3 \right) dx, \end{aligned} \tag{40}$$

where the areas are defined by
$A_1 = \frac{1}{2}(t_2(P) - 1)$
$A_2 = \frac{1}{2}(t_5(P) + t_4 - t_2 - 1)$
$A_3 = \frac{1}{2}(t_5(P) - t_4)$
and $T = t_5$, as in Figure 18.

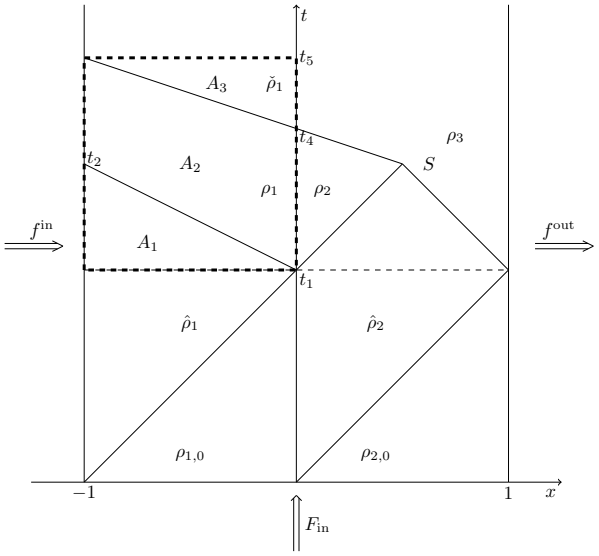

Figure 18: Area of integration in the case $P_1 \leq P < \bar{P}$

- $\bar{P} \leq P \leq P_2$

The TWT_{loc} is as in (39), since it does not depend on the wave interactions but only on the queue length. The $TTT_{loc}(T)$ is given by the constant term plus

$$\begin{aligned} TTT_{loc}(T,P) = &\iint_{A_1+A_2+A_5} \hat{\rho}_1 dtdx + \iint_{A_3} \rho_1(P) dtdx + \iint_{A_4+A_6+A_7} \check{\rho}_1(P) dtdx \\ &+ \int_{t_1}^{t_4} ((F_{\text{in}} - (1-P) f^{\max}))(t-1)) \, dt + T \int_0^1 \left(\check{\rho}_1(P) + \rho_3 \right) dx \\ &+ \int_{t_4}^{T} \left(l(t_4) + \left(F_{\text{in}} - (1-P) f^{\text{out}} \right) (t-t_4) \right) dt \\ &+ T l(t_4) + T \left(F_{\text{in}} - (1-P) f^{\text{out}} \right) (T-t_4). \end{aligned} \tag{41}$$

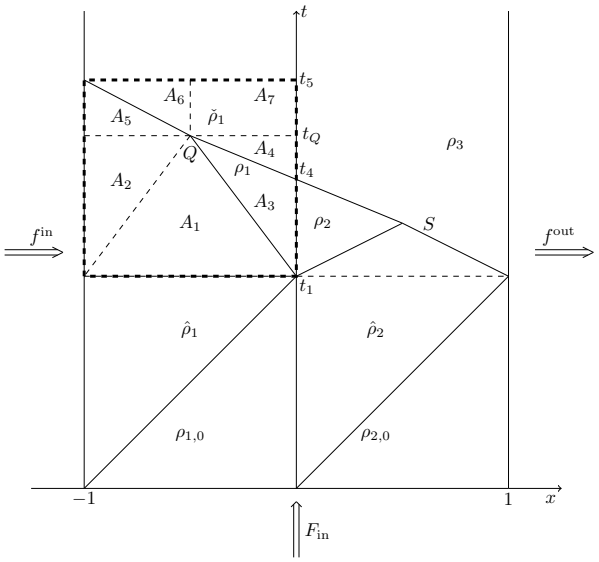

Figure 19: Area of integration in the case $\bar{P} \leq P \leq P_2$

The areas are defined by
$A_1 = \frac{1}{2}(t_Q(P) - 1)$,
$A_2 = \frac{1}{2}(t_Q(P) - 1)(x_Q(P) + 1)$,
$A_3 = \frac{1}{2}(x_Q(P) - x_Q(P)t_4)$,
$A_4 = \frac{1}{2}(t_Q(P) - t_4)(-x_Q(P))$,
$A_5 = \frac{1}{2}(t_5(P) - t_Q(P))(x_Q(P) + 1)$,
$A_6 = \frac{1}{2}(t_5(P) - t_Q(P))(x_Q(P) + 1)$,
$A_7 = (t_5(P) - t_Q(P))(-x_Q(P))$ as in Figure 19.

- $P > P_2$

In this case we have to consider two different situations according to the value of P. If $P > \bar{\bar{P}}$ and $(1-\beta)f^{\text{in}} < f^{\text{out}}$ then the functionals do not depend on P and hence, we skip it from our analysis. If $P_2 < P < \bar{\bar{P}}$ and $(1-\beta)f^{\text{in}} < f^{\text{out}}$ or $(1-\beta)f^{\text{in}} \geq f^{\text{out}}$ then the TWT_{loc} is given by

$$\begin{aligned} TWT_{loc}(T,P) = &\int_{t_1}^{t_4} \left(F_{\text{in}} + (1-\beta)f^{\text{in}} - f^{\max})(t-1)\right) dt \\ &+ \int_{t_4}^{T} \left((F_{\text{in}} + (1-\beta)f^{\text{in}} - f^{\max})(t_4 - 1) + \left(F_{\text{in}} - (1-P)f^{\text{out}}\right)(t - t_4)\right) dt \\ &+ T(F_{\text{in}} + (1-\beta)f^{\text{in}} - f^{\max})(t_4 - 1) + T\left(F_{\text{in}} - (1-P)f^{\text{out}}\right)(T - t_4). \end{aligned} \tag{42}$$

The $TTT_{loc}(T)$, as usual, is instead calculated by the constant term plus

$$\begin{aligned} TTT_{loc}(T,P) = &\int_{A_1} \hat{\rho}_1(P)dtdx + \int_{A_2} \check{\rho}_1(P)dtdx \\ &+ \int_{t_1}^{t_4} \left(F_{\text{in}} + (1-\beta)f^{\text{in}} - f^{\max})(t-1)\right) dt + T\int_0^1 (\check{\rho}_1(P) + \rho_3)\, dx \\ &+ \int_{t_4}^{T} \left((F_{\text{in}} + (1-\beta)f^{\text{in}} - f^{\max})(t_4 - 1) + \left(F_{\text{in}} - (1-P)f^{\text{out}}\right)(t - t_4)\right) dt \\ &+ T(F_{\text{in}} + (1-\beta)f^{\text{in}} - f^{\max})(t_4 - 1) + T\left(F_{\text{in}} - (1-P)f^{\text{out}}\right)(T - t_4) \end{aligned} \tag{43}$$

and the areas for this case are $A_1 = \frac{1}{2}(t_5(P) - t_4)$ and $A_2 = \frac{1}{2}(t_5(P) - t_4)$ as shown in the Figure 20.

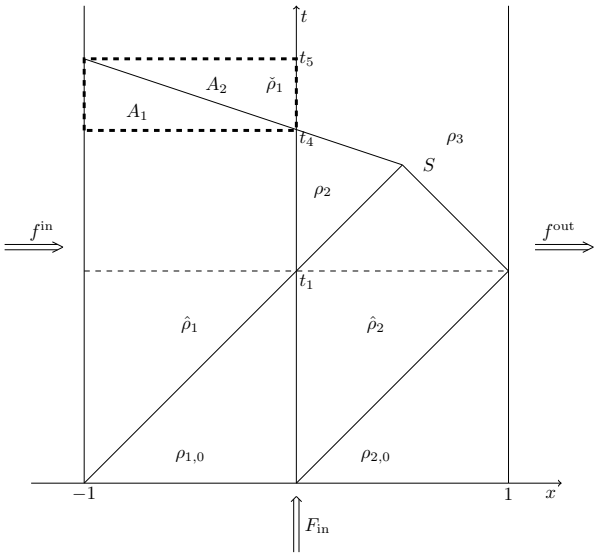

Figure 20: Area of integration in the case $P > P_2$

- $P < P_1$

  We have two different situations which depend on the intersection of the waves as explained in Section 4.2.3. When the waves do not interact between $x = -1$ and $x = 0$ then the TWT_{loc} is computed as

$$TWT_{loc}(T,P) = \int_{t_4}^{T} \left(F_{\text{in}} - (1-P)f^{\text{out}}\right)(t-t_4)dt + T\left(F_{\text{in}} - (1-P)f^{\text{out}}\right)(T-t_4), \tag{44}$$

  while the $TTT_{loc}(T,P)$ is given by

$$\begin{aligned} TTT_{loc}(T,P) = &\iint_{A_1} \rho_1 dtdx + \iint_{A_2} \check{\rho}_1(P)dtdx + \int_{t_4}^{T} \left(F_{\text{in}} - (1-P)f^{\text{out}}\right)(t-t_4)dt \\ &+ T\left(F_{\text{in}} - (1-P)f^{\text{out}}\right)(T-t_4) + T\int_0^1 \left(\check{\rho}_1(P) + \rho_3\right)dx, \end{aligned} \tag{45}$$

  where $A_1 = \frac{1}{2}(t_5 - t_4) = A_2$ as shown in Figure 21.

Whereas when the waves interact between $x = -1$ and $x = 0$ then the TWT is computed does not change and the $TTT_{loc}(T,P)$ is computed as follows

$$\begin{aligned} TTT_{loc}(T,P) = &\iint_{A_1} \hat{\rho}_1 dtdx + \iint_{A_2+A_3+A_4} \check{\rho}_1(P)dtdx \\ &+ \int_{t_4}^{T} \left(F_{\text{in}} - (1-P)f^{\text{out}}\right)(t-t_4)dt + T\left(F_{\text{in}} - (1-P)f^{\text{out}}\right)(T-t_4) + T\int_0^1 \left(\check{\rho}_1(P) + \rho_3\right)dx. \end{aligned}$$

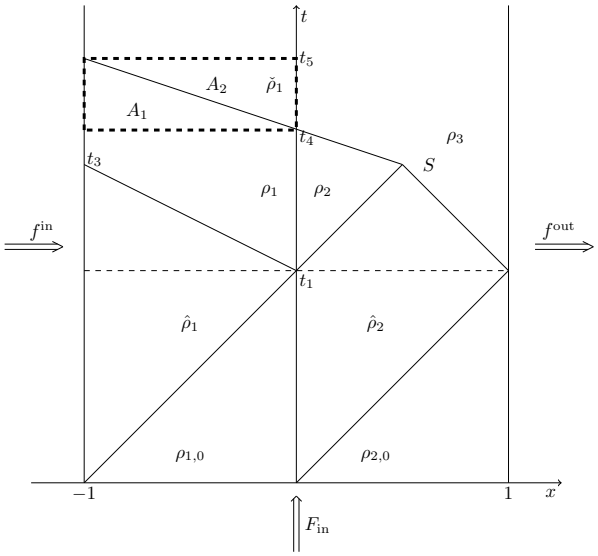

Figure 21: Area of integration in the case $P < P_1$

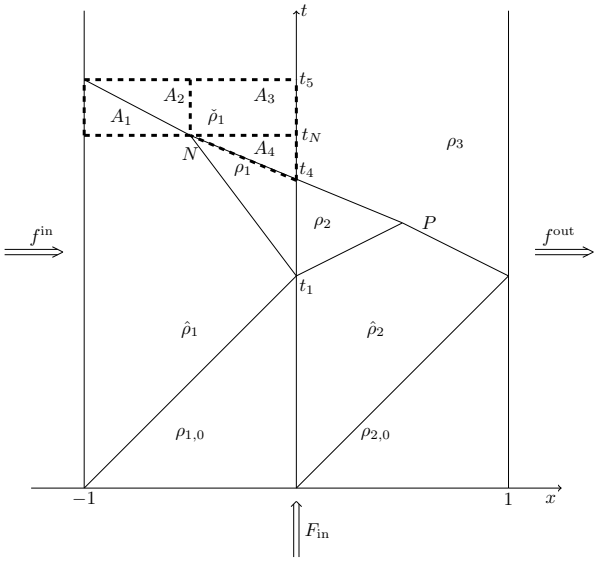

Figure 22: Area of integration when the wave collide in the region [-1,0].

The areas are defined by
$A_1 = A_2 = \frac{1}{2}(t_5(P) - t_N(P))(x_N(P) + 1)$,
$A_3 = (t_5 - t_N(P))(-x_N(P))$,
$A_4 = \frac{1}{2}(t_N(P) - t_4)(-x_N(P))$ as in Figure 22.

5 Numerical Scheme

In this section we consider the traffic regulation problem for a network as the one in Figure 1. We analyze the cost functionals introduced in the previous section. In particular, we want to compare the costs corresponding to the instantaneous optimal choice of the right of way parameter and a fixed constant parameter.

5.1 Network topology

The roundabout will be modeled by:

- 4 roads from the circle: $\mathcal{I}_1, \mathcal{I}_2, \mathcal{I}_3, \mathcal{I}_4$ with $\mathcal{I}_1$ and $\mathcal{I}_4$ linked with periodic boundary conditions;
- 3 roads connecting the roundabout with the rest of the network: 3 incoming lanes and 3 outgoing ones.

5.2 Numerical scheme

From the topology, it can be noted that all the junctions in the roundabout can be represented by 2x2 junctions for which it might be necessary to define a right of way parameter P. The first step is then to discretize the junction model. We define a numerical grid in $(0,T)\times\mathbb{R}$ using the following notation:

- Δx is the fixed space grid size;
- Δt^n is the grid size, given by the CFL condition;
- $(t^n, x_j) = (t^{n-1} + \Delta t^n, j\Delta x)$ for $n \in \mathbb{N}$ and $j \in \mathbb{Z}$ are the grid points.

5.3 Godunov Scheme

The Godunov scheme as introduced in [16] is based on exact solutions to Riemann problems. The main idea of this method is to approximate the initial datum by a piecewise constant function, then the corresponding Riemann problems are solved exactly and a global solution is simply obtained by piecing them together. Finally, one takes the mean on the cell and proceeds by induction. Under the CFL condition

$$\Delta t^n \max_{j\in\mathbb{Z}} \left|\lambda^n_{j+\frac{1}{2}}\right| \leq \frac{1}{2}\Delta x, \tag{46}$$

the waves generated by different Riemann problems do not interact. Above, $\lambda^n_{j+\frac{1}{2}}$ is the wave speed of the Riemann problem solution at the interface $x_{j+\frac{1}{2}}$ at time t^n. Under the condition (46) the scheme can be written as

$$v_j^{n+1} = v_j^n - \frac{\Delta t^n}{\Delta x}(g(v_j^n, v_{j+1}^n) - g(v_{j-1}^n, v_j^n)), \tag{47}$$

where the numerical flux g takes in general the following expression:

$$g(u,v) = \begin{cases} \min_{z\in[u,v]} f(z) & \text{if } u \leq v, \\ \max_{z\in[v,u]} f(z) & \text{if } v \leq u. \end{cases} \tag{48}$$

5.3.1 Conditions at the Junction.

Each road is divided in J + 1 cells numbered from 0 to J. For the incoming main lane, that is connected at the junction at the right endpoint, we set

$$v_J^{n+1} = v_J^n - \frac{\Delta t^n}{\Delta x}(\hat{\Gamma}_1 - g(v_{J-1}^n, v_J^n)),$$

while for the outgoing one, connected at the junction at the left endpoint, we have

$$v_0^{n+1} = v_0^n - \frac{\Delta t^n}{\Delta x}(g(v_0^n, v_1^n) - \hat{\Gamma}_2),$$

where $\hat{\Gamma}_1$ and $\hat{\Gamma}_2$ are the maximized fluxes computed in Section 3.

5.4 ODE Treatment

Let us consider now the buffer modeled by the ODE (2). At each time step $t^n = t^{n-1} + \Delta t^n$ we compute the new value of the queue length with explicit Euler first order integration:

1. If $F_{\text{in}}(t^n) < \hat{\Gamma}_{\text{r1}}$

$$l^{n+1} = \begin{cases} l^n + (F_{\text{in}}(t^n) - \hat{\Gamma}_{\text{r1}})\Delta t^n & \text{for } t^{n+1} < \bar{t}, \\ 0 & \text{otherwise .} \end{cases}$$

2. If $F_{\text{in}}(t^n) \geq \hat{\Gamma}_{\text{r1}}$

$$l^{n+1} = l^n + (F_{\text{in}}(t^n) - \hat{\Gamma}_{\text{r1}})\Delta t^n.$$

For more details on the numerical scheme for the junction model we refer the reader to [5].

6 Numerical Simulations

In this section we show some simulations results corresponding to different choices of the right of way parameters. We consider approximations obtained by Godunov numerical method, with space step $\Delta x = 0.1$ and the time step determined by the CFL condition. The traffic flow on the road network is simulated in a time interval $[0, T]$, where $T = 50$. As for the initial condition on the roads of the network, we assume that at initial time $t = 0$ all the roads and the buffers are empty, $f^{\text{in}} = f^{\text{out}} = 0$ and we take $F_{\text{in}} \neq 0$. We consider the following parameters for each link: $f^{\max} = 0.66$, $\rho_{cr} = 0.66$ and $\gamma_{r1}^{\max} = 0.65$. Moreover, we distinguish different cases of simulations which vary according to the value of $F_{\text{in}} \in \{0.1, 0.2, 0.3, 0.4, 0.5, 0.6\}$ and $\beta \in \{0.2, 0.3, 0.4, 0.5, 0.6, 0.7\}$. For each value of F_{in} and β we study different simulations cases:

- Instantaneous right of way parameter that optimizes the cost functionals TTT_{loc} and TWT_{loc}. Given the complicated expressions of the cost functionals it is difficult to use an analytical approach for the development of an optimized algorithm for the whole roundabout. For this reason, we consider at each junction and at each time step the optimal parameters corresponding to the road densities near the junction. The technique for the simulation of the optimal case is based on the local optimization of every junction of $2x2$ type, which form the roundabout. To compute the cost functionals, at each time step the values of F_{in}, f^{out} and f^{in} are found as follows:
  - $f^{\text{in}} = \delta(\rho_{inc})$
  - $f^{\text{out}} = \sigma(\rho_{out})$
  - $F_{\text{in}} = d(F_{\text{in}}, l^n)$

  The optimal value of the priority parameter is then computed exactly (i.e. analytically as explained in 4) at each time step for the corresponding input values.
- Fixed right of way parameter. We analyze the behavior of the cost functionals, assuming that the priority parameter P is the same and kept fixed for each junction.

7 Simulation Results

In Figures 24 and 23 we show some of the simulation results for some representative cases. More precisely we show the value of the functionals TTT (13) and TWT (14) computed on the whole roundabout as a function of F_{in}. A legend for every picture indicates the different simulation cases. Moreover, the tables 1, 2, 3, 4, 5 and 6 depict the gain in percentage between the optimal case and the constant one for different values of P.

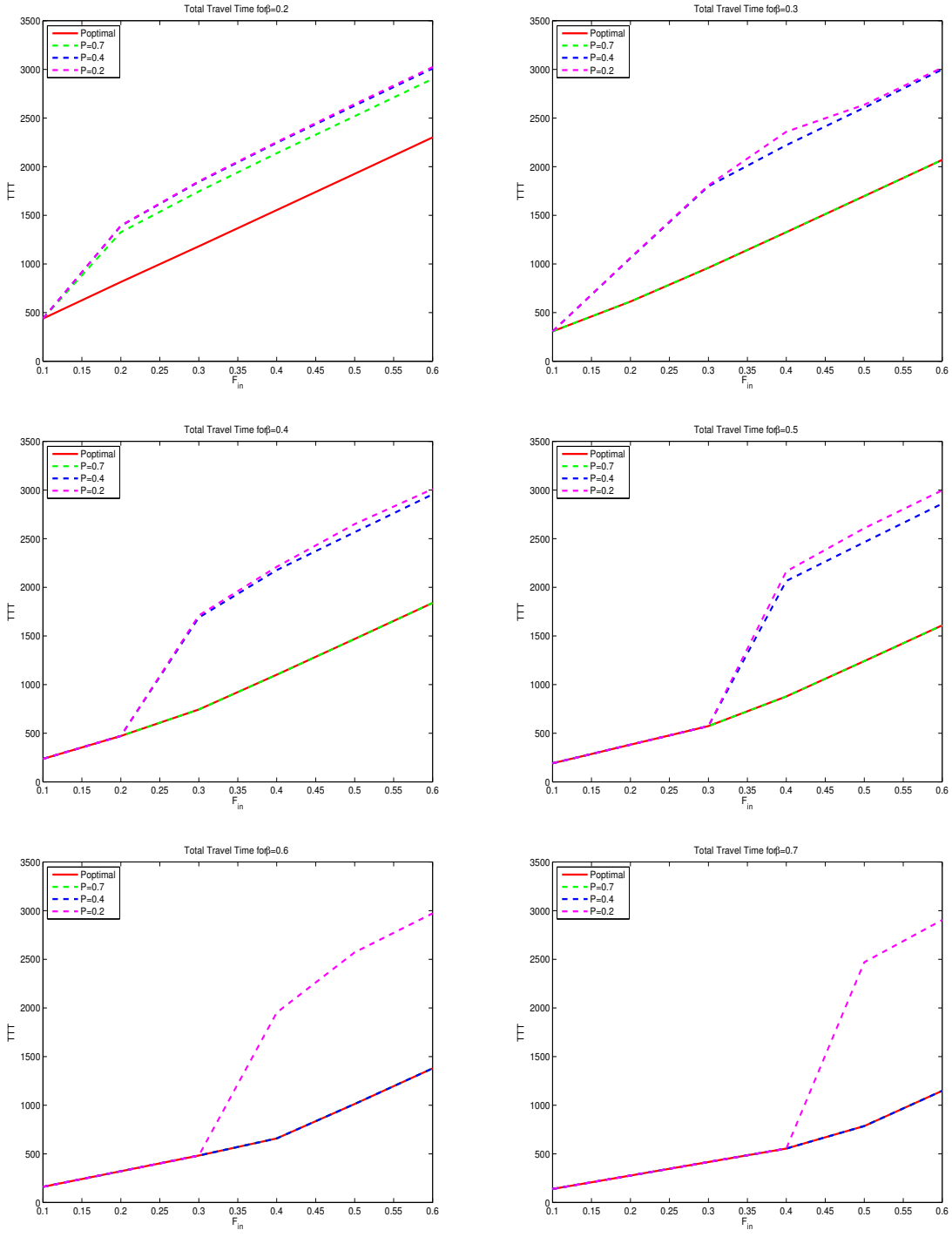

Figure 23: TTT as a function of F_{in} computed for a time horizon $T = 50$.

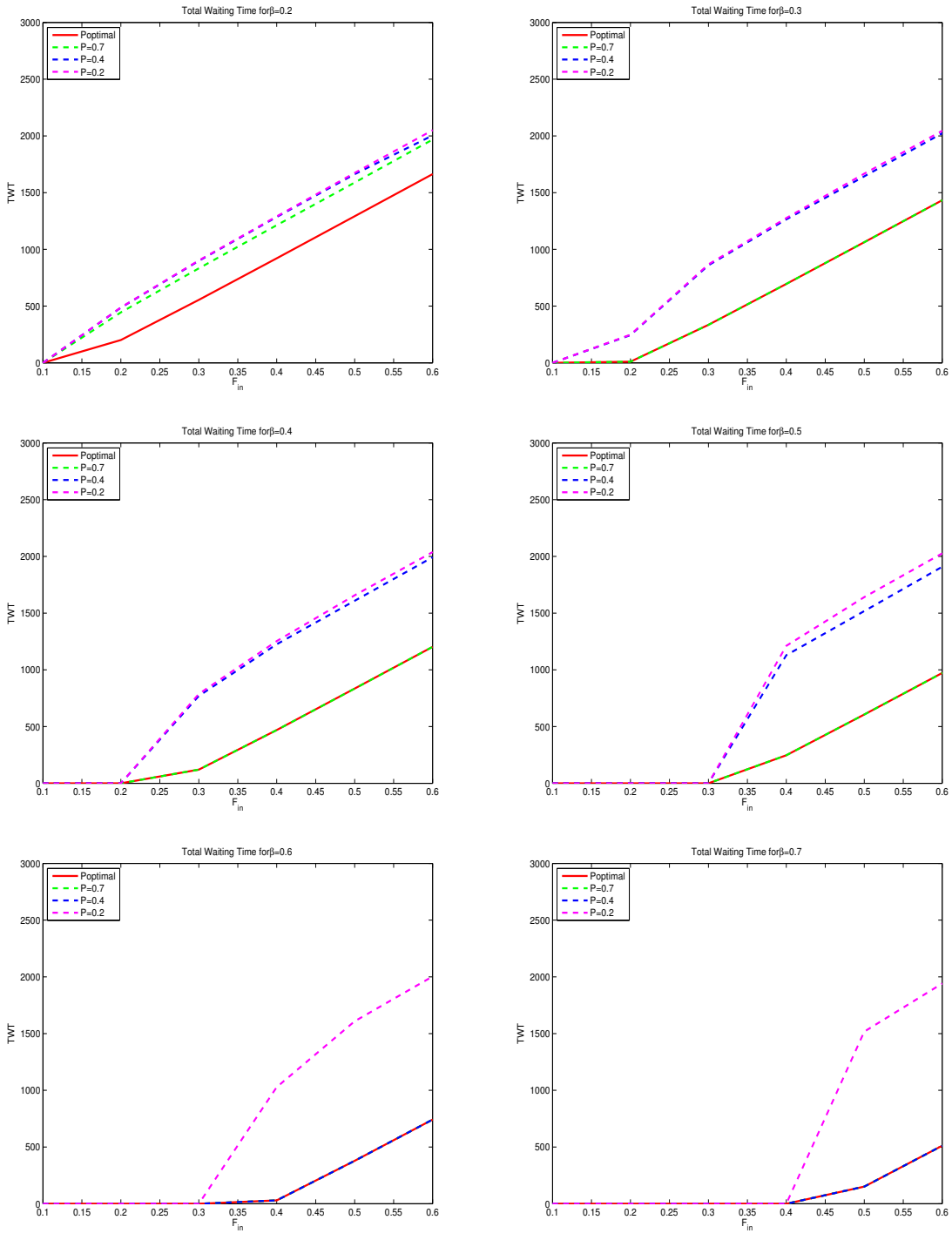

Figure 24: TWT as a function of F_{in} computed for a time horizon $T = 50$.

F_{in} \ β	0.2	0.3	0.4	0.5	0.6	0.7
0.1	0.0000%	0.0000%	0.0000%	0.0000%	0.0000%	0.0000%
0.2	-23.9359%	0.0000%	0.0000%	0.0000%	0.0000%	0.0000%
0.3	-19.2538%	0.0000%	0.0000%	0.0000%	0.0000%	0.0000%
0.4	-15.8362%	0.0000%	0.0000%	0.0000%	0.0000%	0.0000%
0.5	-13.3060%	0.0000%	0.0000%	0.0000%	0.0000%	0.0000%
0.6	-11.5724%	0.0000%	0.0000%	0.0000%	0.0000%	0.0000%

Table 1: Gain in TTT computed with the optimal right of way parameter and a fixed one $P = 0.7$.

F_{in} \ β	0.2	0.3	0.4	0.5	0.6	0.7
0.1	0.0000%	0.0000%	0.0000%	0.0000%	0.0000%	0.0000%
0.2	-26.1638%	-26.7080%	0.0000%	0.0000%	0.0000%	0.0000%
0.3	-21.8880%	-30.3638%	-38.8852%	0.0000%	0.0000%	0.0000%
0.4	-18.2182%	-25.1910%	-32.8044%	-40.3677%	0.0000%	0.0000%
0.5	-15.3961%	-21.1096%	-27.1844%	-32.9931%	0.0000%	0.0000%
0.6	-13.3412%	-18.3294%	-23.2688%	-27.9928%	0.0000%	0.0000%

Table 2: Gain in TTT computed with the optimal right of way parameter and a fixed one $P = 0.4$.

F_{in} \ β	0.2	0.3	0.4	0.5	0.6	0.7
0.1	0.0000%	0.0000%	0.0000%	0.0000%	0.0000%	0.0000%
0.2	-26.2608%	-26.9396%	0.0000%	0.0000%	0.0000%	0.0000%
0.3	-22.0246%	-30.6028%	-39.4182%	0.0000%	0.0000%	0.0000%
0.4	-18.3772%	-28.0082%	-33.4924%	-42.2899%	-49.5546%	0.0000%
0.5	-15.6867%	-21.6484%	-28.6658%	-35.5027%	-43.4925%	-51.7438%
0.6	-13.5821%	-18.6328%	-24.1359%	-30.1316%	-36.6248%	-43.3260%

Table 3: Gain in TTT computed with the optimal right of way parameter and a fixed one $P = 0.2$.

F_{in} \ β	0.2	0.3	0.4	0.5	0.6	0.7
0.1	0.0000%	0.0000%	0.0000%	0.0000%	0.0000%	0.0000%
0.2	-37.7363%	0.0000%	0.0000%	0.0000%	0.0000%	0.0000%
0.3	-20.0221%	0.0000%	0.0000%	0.0000%	0.0000%	0.0000%
0.4	-13.6862%	0.0000%	0.0000%	0.0000%	0.0000%	0.0000%
0.5	-10.3010%	0.0000%	0.0000%	0.0000%	0.0000%	0.0000%
0.6	-8.3728%	0.0000%	0.0000%	0.0000%	0.0000%	0.0000%

Table 4: Gain in TWT computed with the optimal right of way parameter and a fixed one $P = 0.7$.

F_{in} \ β	0.2	0.3	0.4	0.5	0.6	0.7
0.1	0.0000%	0.0000%	0.0000%	0.0000%	0.0000%	0.0000%
0.2	-41.5096%	-92.2568%	0.0000%	0.0000%	0.0000%	0.0000%
0.3	-23.6510%	-43.9810%	-72.9952%	0.0000%	0.0000%	0.0000%
0.4	-16.5219%	-29.0594%	-44.6035%	-64.1409%	0.0000%	0.0000%
0.5	-12.5626%	-21.4584%	-31.6873%	-42.9263%	0.0000%	0.0000%
0.6	-9.2872%	-17.0847%	-24.7253%	-32.5150%	0.0000%	0.0000%

Table 5: Gain in TWT computed with the optimal right of way parameter and a fixed one $P = 0.4$.

F_{in} \ β	0.2	0.3	0.4	0.5	0.6	0.7
0.1	0.0000%	0.0000%	0.0000%	0.0000%	0.0000%	0.0000%
0.2	-41.6784%	-92.3688%	0.0000%	0.0000%	0.0000%	0.0000%
0.3	-23.8452%	-44.3239%	-73.5147%	0.0000%	0.0000%	0.0000%
0.4	-16.7143%	-29.4949%	-45.5005%	-66.1746%	-94.3553%	0.0000%
0.5	-12.8840%	-22.1229%	-33.0143%	-46.0431%	-61.9339%	-81.8636%
0.6	-10.4278%	-17.6115%	-25.7892%	-35.1576%	-45.9640%	-58.3022%

Table 6: Gain in TWT computed with the optimal right of way parameter and a fixed one $P = 0.2$.

In both cases, the cost functionals computed with a fixed right of way parameter or with the optimal ones have a different behavior only for those values of F_{in} for which the problem is supply limited. In both cases we have better results for the optimal case. We can see that even when optimizing the TWT, low values of the priority parameters that should favor the entrance with the respect to the main lane are a bad choice. In fact, for these values the roundabout tends to be overly congested blocking, as a matter of fact, the entrances. From our analysis, it seems that in both cases the optimal priority parameters are the ones that favors the main lane compared to the entrances.

8 Conclusions

In this paper we consider the optimization of road traffic on roundabouts. We treat the roundabout as a concatenation of $2x2$ junctions. We solve an optimization problem where the optimal control acts on the priority parameters, which assign right of way among incoming roads, for example through traffic lights. Two cost functionals are introduced, measuring the total waiting time and total travel time. We compute analytically the cost functionals for a single junction, and find the control parameters that locally optimize the flow. The approach is tested on a simple roundabout with three incoming and three outgoing roads. Two different choices of parameters are considered: instantaneusly locally optimal and fixed. The local optima outperform the other choice, improving the performances of the network.

Acknowledgments

This research was supported by the European Research Council under the European Union's Seventh Framework Program (FP/2007-2013) / ERC Grant Agreement n. 257661 and by "*International Science Program, Sweden*" (ISP) and "*African Mathematics Millennium Science Initiative*" (AMMSI).

References

[1] Lighthill M J, Whitham B. 1955. *On kinematic waves II. A theory of traffic flow on crowded roads.* Proceedings of the Royal Society of London Series A, **229** 317 - 346.

[2] Richards P I. 1956. *Shock waves on the highways*. Operations Research, **4** 42 - 51.

[3] Coclite G M, Garavello M, Piccoli B. 2005. *Traffic flow on a road network*. SIAM Journal of Mathematical Analysis, **36**(6) 1862 - 1886.

[4] Colombo R M, Goatin P, Piccoli B. 2010. *Road network with phase transition*. Journal of Hyperbolic Differential Equations, **07**(2010) 85 - 106.

[5] Delle Monache M L,Reilly J, Samaranayake S, Krichene W, Goatin P, Bayen A M. 2013. *A PDE-ODE model for a junction with ramp buffer*. SIAM Journal of Applied Mathematics, to appear.

[6] Garavello M, Goatin P. 2012. *The Cauchy problem at a node with a buffer*. Discrete and Continuous Dynamical Systems Series A, **32**(6) 1915 - 1938.

[7] Cascone A, D'Apice C, Piccoli B, Raritˆa L. 2007. *Optimization of traffic on road networks*. Mathematical Models and Methods in Applied Sciences, **17**(10) 1587 - 1617.

[8] Chitour Y, Piccoli B. 2005. *Traffic circles and timing of traffic lights for cars flow*. Discrete and Continuous Dynamical Systems Series B, **5**(3) 599.

[9] Cutolo A, D'Apice C, Manzo R. 2011. *Traffic optimization at junctions to improve vehicular flows*. International Scholarly Research Network, 19 pp.

[10] Gugat M, Herty M, Klar A, Leugering G. 2005. *Optimal control for traffic flow networks*. Journal of optimization theory and applications, **126**(3) 589 - 616.

[11] Herty M, Klar A. 2003. *Modeling, simulation, and optimization of traffic flow networks*. SIAM Journal on Scientific Computing, **25**(3) 1066 - 1087.

[12] Bressan A. 2000. *Hyperbolic systems of conservation laws. The one-dimensional Cauchy problem*. Oxford University Press.

[13] Kružhkov S N. 1970. *First order quasilinear equations with several independent variables*. Mat. Sb. (N.S.), **81**(123) 228 - 255.

[14] Garavello M, Piccoli B. 2006. *Traffic Flow on Networks: Conservation Laws Model*. AIMS Series on Applied Mathematics. American Institute of Mathematical Sciences.

[15] Obsu L L, Delle Monache M L, Goatin P, Kasa S M. 2013. *Macroscopic traffic flow optimization on roundabouts*. Inria Research Report N 8291, http://hal.inria.fr/hal-00818208.

[16] Godunov S K. 1959. *A finite difference method for the numerical computation of discontinuous solutions of the equations of fluid dynamics*. . Matematicheskii Sbornik, **47** 271 - 290.

[17] Bardos C, Le Roux A Y, Nédélec J C. 1979. *First order quasilinear equations with boundary conditions*. Comm. Partial Differential Equations, **4**(9) 1017 - 1034.

[18] LeFloch P. 1988. *Explicit formula for scalar non-linear conservation laws with boundary condition*. Mathematical Methods in the Applied Sciences, **10**(3) 265 - 287.

[19] Leveque R J. 1992. *Numerical methods for conservation laws.*. Lectures in mathematics ETH Zürich.